Pan-cancer analysis reveals the potential role of DHCR24 in bladder cancer via interactions with HRAS to facilitate cholesterol synthesis

ZHIBIN WANG[1], JING MAO[1], YUKUN ZHANG[1], WENYU YANG[1], DELIANG SUN[1], ZIYIN LU[1], XIULI LU[1] and BING GAO[2]

[1]Department of Biochemistry and Cell Biology, School of Life Sciences, Liaoning University, Shenyang, Liaoning 110036, P.R. China; [2]Department of Cell Biology and Genetics, School of Basic Medical Sciences, Shenyang Medical College, Shenyang, Liaoning 110034, P.R. China

Received January 14, 2025; Accepted May 14, 2025

DOI: 10.3892/ol.2025.15131

Abstract. There is a strong association between cholesterol reprogramming and cancer development. However, 3β-hydroxysteroid Δ24-reductase (DHCR24), the final enzyme in the cholesterol biosynthesis pathway, has been relatively understudied in cancer progression. The present study aimed to perform a comprehensive pan-cancer analysis of DHCR24 to elucidate its role across different malignancies. The interacting proteins of DHCR24 were identified by molecular docking node dynamics simulation. Duolink proximity ligation, cell viability and filipin staining assays were used to assess the function of DHCR24 in cancer cells and its underlying oncogenic mechanisms. The findings revealed that DHCR24 exhibits high expression in seven cancer types (bladder cancer, breast invasive carcinoma, liver hepatocellular carcinoma, prostate adenocarcinoma, cervical squamous cell carcinoma and endocervical adenocarcinoma, uterine corpus endometrial carcinoma and stomach adenocarcinoma), and low expression in five others (glioblastoma multiforme, kidney chromophobe, kidney renal clear cell carcinoma, lung adenocarcinoma and lung squamous cell carcinoma), suggesting that DHCR24 serves distinct roles depending on the cancer type. Notably, it was demonstrated that DHCR24 expression consistently increases with tumor stage and serves as an independent prognostic factor in BLCA. Moreover, molecular docking and kinetic modeling identified HRAS as a key interacting protein of DHCR24. The Duolink assay further demonstrated that DHCR24 interacts with HRAS outside the nucleus in 5637 human BLCA cells. Filipin fluorescence staining and cell proliferation assays also revealed that this interaction promoted cholesterol synthesis, contributing to cancer cell proliferation in the 5637 cells. In conclusion, the results of the present study provide novel insights into the oncogenic role of DHCR24 in BLCA and demonstrates its interaction with HRAS for the first time to the best of our knowledge, highlighting a potential mechanism driving tumor progression.

Correspondence to: Professor Bing Gao, Department of Cell Biology and Genetics, School of Basic Medical Sciences, Shenyang Medical College, 146 Huanghe North Street, Shenyang, Liaoning 110034, P.R. China
E-mail: gaobingdr@hotmail.com

Professor Xiuli Lu, Department of Biochemistry and Cell Biology, School of Life Sciences, Liaoning University, 66 Chongshan Middle Road, Huanggu, Shenyang, Liaoning 110036, P.R. China
E-mail: luxiuli@lnu.edu.cn

Abbreviations: CRC, colorectal cancer; DHCR24, 3β-hydroxysteroid Δ24-reductase; TIMER, Tumor Immune Estimation Resource; TPM, transcripts per million; OS, overall survival; DFS, disease-free survival; BLCA, bladder cancer; GO, Gene Ontology; KEGG, Kyoto Encyclopedia of Genes and Genomes; PPI, protein-protein interaction; EGF, epidermal growth factor; BRCA, breast cancer; LUSC, lung squamous cell carcinoma; TME, tumor microenvironment; TCGA, The Cancer Genome Atlas

Key words: DHCR24, pan-cancer analysis, BLCA, HRAS, cholesterol synthesis

Introduction

Genetic alterations accumulating in cancer cells give rise to novel tumor-associated antigens, which serve as key hallmarks of tumor progression (1). As a result, oncology research has shifted towards precision oncology, where treatment strategies are customized to target specific molecular abnormalities in individual patients with different cancer types (2,3).

Hyperlipidemia is a well-recognized, independent risk factor for atherosclerotic diseases such as stroke and myocardial infarction. It has also been linked to several other major disorders, including cancer (4). Tumor metabolic reprogramming refers to a series of metabolic shifts caused by structural and functional changes in key oncogenes and tumor suppressors, enabling cancer cells to sustain growth and adapt to unfavorable microenvironments (5). Among these metabolic adaptations, cholesterol metabolism serves a fundamental role. Cancer cells rely heavily on cholesterol for uncontrolled proliferation and survival, and they can reprogram cholesterol

homeostasis by increasing uptake, dysregulating biosynthetic pathways, reducing efflux and accumulating cholesterol in lipid droplets to regulate critical signaling pathways (6).

Emerging evidence underscores the pivotal role of cholesterol in tumor initiation, progression and metastasis. Several studies have reported a positive association between elevated serum cholesterol levels and increased cancer risk and aggressiveness (7). High circulating cholesterol levels have also been associated with an increased risk of developing prostate cancer, whereas cholesterol-lowering interventions have been suggested to confer protective effects (8). Moreover, cholesterol has been implicated in rectal cancer progression, where excessive cholesterol promotes the degradation of squalene epoxidase, a rate-limiting enzyme in cholesterol biosynthesis. Notably, reduced squalene epoxidase expression has been associated with invasive colorectal cancer (CRC) (9). In breast cancer (BRCA), cholesterol contributes to metastasis through its oxidative metabolite, 27-hydroxycholesterol, which is induced by a high-fat diet. Notably, eliminating or inhibiting the enzymes responsible for this metabolite markedly reduces cancer metastasis in animal models (10). Furthermore, 3β-hydroxysteroid Δ24-reductase (DHCR24) promotes lymphangiogenesis and lymph node metastasis in bladder cancer (BLCA), both *in vitro* and *in vivo* (11).

Cholesterol synthesis is mainly carried out through the Bloch pathway, and DHCR24 is the key enzyme in its final step, in humans and hamsters (12). Our previous research in a mouse model demonstrated that a high-fat diet induces brain injury and neuronal apoptosis by downregulating DHCR24 (13). Furthermore, suppressing DHCR24 expression has been reported to inhibit the proliferation and metastasis of multiple cancer cell types. For example, the anticancer peptide Q7 downregulates DHCR24, thereby disrupting lipid raft formation and subsequently inhibiting the AKT signaling pathway in human endometrial cancer cells, leading to reduced tumorigenicity, proliferation and migration (14). Similarly, DHCR24 is essential for cholesterol biosynthesis and lipid raft formation, and its inhibition by Genkwadaphnin has been reported to effectively suppress the growth and invasion of hepatocellular carcinoma cells (15). Additionally, methotrexate resistance in gestational trophoblastic neoplasia cells has been associated with DHCR24-mediated cholesterol biosynthesis (16).

Despite its crucial role in cholesterol metabolism and the growing body of evidence suggesting that DHCR24 inhibition suppresses tumor proliferation and metastasis, a comprehensive pan-cancer analysis of DHCR24 is lacking. Therefore, the present study aimed to perform an extensive pan-cancer analysis of DHCR24 and experimentally elucidate its oncogenic role and underlying mechanisms in BLCA.

Materials and methods

Tumor immune estimation resource (TIMER). The DHCR24 expression profile and the abundance of immune infiltrates in pan-cancer were analyzed using the TIMER database (https://cistrome.shinyapps.io/timer/). The gene expression levels are represented as $\log_2$ [transcripts per million (TPM)] values (17).

DHCR24 expression pattern in human pan-cancer. The difference in the expression of DHCR24 between tumor and adjacent normal tissues was assessed for the different tumors or specific tumor subtypes of The Cancer Genome Atlas (TCGA) project (https://www.cancer.gov/ccg/research/genome-sequencing/tcga/studied-cancers). R version 4.1.2 (The R Foundation) was used for analysis, and specific R package, including limma 3.64.0 (https://bioinf.wehi.edu.au/limma/) and ggplot2 3.5.2 (https://ggplot2.tidyverse.org) were utilized. Additionally, violin plots were generated for DHCR24 expression levels in different pathological stages (stages I-IV) of all TCGA tumors via the 'Pathological Stage Plot' module of GEPIA2.0 (http://gepia2.cancer-pku.cn/). The $\log_2$(TPM+1) transformed expression data were applied for the box or violin plots.

Prognostic analysis. The 'Survival Map' module of GEPIA2.0 (http://gepia2.cancer-pku.cn/) was used to obtain the overall survival (OS) and disease-free survival (DFS) significance map data of DHCR24 across all TCGA tumors. Cutoff-high (50%) and -low (50%) values were used as the expression thresholds for splitting the high- and low-expression cohorts. The log-rank test was used in the hypothesis test, and the survival plots were also obtained using the 'Survival Analysis' module of GEPIA2.0 (http://gepia2.cancer-pku.cn/). Moreover, to assess whether the acquired genes were associated with the survival of patients with BLCA, univariate and multifactorial proportional hazards model (COX) analyses were performed. Subsequently, the survival of patients with cancer was predicted and further assessed using a nomogram and receiver operating characteristic (ROC) curve analysis.

Differential gene enrichment analysis. Co-expression analysis of the differential genes obtained from the analysis in BLCA was performed. Subsequently, Gene Ontology (GO) and Kyoto Encyclopedia of Genes and Genomes (KEGG) enrichment analysis, as well as gene set enrichment analysis were performed on the differential genes.

Immuno-infiltration analysis. The expression data of patients with BLCA was analyzed for immune infiltration, immune checkpoint and tumor mutation load. R version 4.1.2 was used for analysis, with the R packages reshape2 1.4.4 (https://github.com/hadley/reshape) and vioplot 0.5.1 (https://github.com/TomKellyGenetics/vioplot) utilized.

Molecular docking and dynamics simulation. In our preliminary screening study (unpublished data), immunoprecipitation (IP) mass spectrometry using antibodies against DHCR24 as the IP antibody and 293 cells was performed to identify the DHCR24-interaction proteins. In total, 413 proteins were identified as DHCR24-interaction proteins (Table SI). These data were combined with the results of four publicly available protein interaction databases Biogrid (https://thebiogrid.org/) (DHCR24 dataset), GeneMania (http://genemania.org/) (DHCR24 dataset), Unihi (http://193.136.227.168/UniHI/pages/unihiSearch.jsf) (24-Dehydrocholesterol Reductase dataset) and Hitpredict (http://www.hitpredict.org/) (dataset Q15392) to form a DHCR24 candidate interaction proteome containing 492

protein molecules. Furthermore, the enrich Pathway function of Clusterprofiler 3.21 (https://www.bioconductor.org/packages/release/bioc/html/clusterProfiler.html) software of R 4.1.2 software was used to perform enrichment analysis in terms of cellular pathways and to predict the important cellular signaling pathways of DHCR24 and its interacting proteins.

Subsequently, the interacting proteome was entered into STRING 12.0 (https://string-db.org/) to form a protein-protein interaction (PPI) network. The network map was then downloaded and imported into Cytoscape3.9.1 (https://cytoscape.org/). DHCR24 with HRAS, a common variant in cancer, was selected as a node, all proteins adjacent to it were selected to form a new network map, and the network was analyzed. The central node of the PPI network was determined.

Modeller 9.24 software (https://salilab.org/modeller/) was used to screen all sequences with homology of >30% as templates for homology modeling, and the obtained protein structures were optimized for kinetic simulations using gromacs2019.5 (https://manual.gromacs.org/documentation/2019.6/download.html) for 50,000 steps of energy minimization, constant temperature of 300 k, nd 1 nsec, with a Rasch plot of Modeller 9.24 (http://mordred.bioc.cam.ac.uk/~rapper/rampage.php) as a standard for protein structure evaluation. Subsequently, using the biomacromolecular docking platform ZDOCK2.3.2 (http://zdock.umassmed.edu/), the structure of DHCR24 homology modeled with the activated HRAS structure (PDB database, https://www.rcsb.org/; 1HE8 B chain) was submitted separately and docking calculations were performed. The best-bound structural system of the aforementioned DHCR-HRAS complex was determined as the initial conformation, and molecular dynamics simulations were performed using the NAMD 2.13 (https://www.ks.uiuc.edu/Research/namd/2.13/notes.html) program and Amber's ff14SB (Preliminary version; https://pubs.acs.org/doi/10.1021/acs.jctc.5b00255) force field. A 10.0 Å TIP3P water box model was added around the complex and the addition made the system electrically neutral. The complex was slowly warmed by 30,000 steps of initial energy minimization and 1,000 steps of 0-300 K using a constant temperature and constant pressure system. Molecular dynamics simulations of the complexes were performed for 70 nsecs to study the interactions between DHCR24-HRAS complexes, and the results of the molecular dynamics simulation calculations were analyzed using Pymol2.6 software (https://pymol.org/).

Human protein atlas (HPA) database analysis. In order to explore DHCR24 expression in patients with BLCA, data was retrieved from the HPA database (https://www.proteinatlas.org/). The BLCA data and normal bladder data in the DHCR24 immunohistochemistry dataset were analyzed.

Cell culture. For *in vitro* cytological validation, the human BLCA 5637 cell line was used. These cells can produce products such as stem cell factor, interleukin-1, interleukin-6 and granulocyte macrophage-colony stimulating factor. Moreover, 5637 cells were derived from the bladder epithelial cells of a 68-year-old male patient with BLCA which had adherent growth characteristics. The cell line is widely used in the study of the mechanism of BLCA development and drug treatment strategies (18,19).

Human BLCA 5637 cells, purchased from Wuhan Punosai Life Technology Co., Ltd., were seeded at $5x10^6$ cells/well in six-well plates and cultured in 10% FBS/DMEM in a 5% CO_2 incubator at 37˚C. Fetal calf serum and DMEM were purchased from Hyclone, and the Penicillin-Streptomycin Solution mixture was purchased from Donglin Changsheng Biotechnology Co., Ltd. The concentration of double antibody was 1%. When the cells reached ~50% confluence, the old medium was discarded and the cells were starved overnight. Subsequently, 5 ml DMEM was added to each well, images of the cells were captured, and then drug treatment was applied. To observe the number of adherent cells after 72 h, the cells were counted in the same position of each group and each well under the same field of view using the same microscope magnification. U18666A, Filipin, EGF and paraformaldehyde were purchased from Beijing Ding Guo Changsheng Biotechnology Co., Ltd. Lonafarnib was purchased from Selleck Chemicals. The working concentrations of EGF, U18666A and lonafarnib were 15 ng/ml, 2 μM and 1.9 nM, respectively. The inverted and fluorescence microscopes used were manufactured by Olympus Corporation. The number of adherent cells per unit area was plotted using GraphPad Prism 9.3 (Dotmatics).

Cell viability assay. Cells were seeded in 96-well plates at a density of $1x10^5$ cells/well and incubated for 24 h at 37˚C. When the cells reached ~50% confluence, the old medium was discarded and the cells were starved overnight. Next, 0.5 mg/ml tetrazolium salt (MTT) was added and the cells were incubated for 4 h at 37˚C. The working concentrations of EGF, U18666A and lonafarnib were 15 ng/ml, 2 μM and 1.9 nM, respectively. EGF can activate the downstream signaling pathway to promote the proliferation of cancer cells. U18666A is a DHCR24 inhibitor, and the cell viability and proliferation changes after inhibition of DHCR24 can be explored. Lonafarnib, an HARS inhibitor, can be used to investigate the changes in cell viability and proliferation after inhibition of HRAS activity. Several negative control groups were set up, namely the untreated control group and the EGF, U18666A and lonafarnib control groups. The EGF control group was cultured with 15 ng/ml EGF for 15 min and then the medium was replaced. The U18666A control group was treated with 2 μM U18666A, and the lonafarnib control group was treated with 1.9 nM lonafarnib. The other two experimental groups were treated with 15 ng/ml EGF for 15 min, then the medium was replaced, and then 2 μM U18666A and 1.9 nM lonafarnib were added, respectively. After drug addition, all cells were treated at 37˚C for 72 h. Following the incubation period, the formazan crystals were dissolved using 100 μl of dimethyl sulfoxide (Sigma-Aldrich; Merck KGaA). The absorbance of the samples was then measured at 490 nm using a microplate reader (Spark®; Tecan Group, Ltd.). The percentage of viable cells was calculated and compared with that of the negative control.

Duolink. The cells were divided into two groups: One group was cultured with medium containing 15 ng/ml EGF to activate HRAS, whilst the other was cultured with the same amount of medium without EGF as a control. After 15 min, the medium in the wells was discarded, and the cells were eluted with 1 ml PBS per well. A total of 1 ml 4% paraformaldehyde was added

to the cells in each well, and fixed at room temperature for 30 min after agitation at room temperature. The paraformaldehyde was removed by suction, and 1 ml PBS was added to each well for shaking and cleaning for 3x10 min. Blocking was performed using 1 ml PBS containing a final concentration of 1% BSA and 0.3% Triton-PBS, and the mixture was shaken for 1 h at room temperature. Cells were eluted with PBS to wash away residual blocking reagents. A sealing film of a suitable size was cut, absorbent paper and tin foil was put under it, they were placed in a Petri dish to form a wet box and then Round Coverslip piece was transferred to the wet box. A drop of Duolink® Blocking Solution (Sigma-Aldrich; Merck KGaA) was dropped on each slide to ensure complete coverage of the slide, and the slide was incubated at 37˚C for 1 h. Duolink® Antibody Diluent (Sigma-Aldrich; Merck KGaA) was then vortexed to dilute the anti-HRAS [Santa Cruz Biotechnology (Shanghai) Co., Ltd.; cat. no. SC-35] and anti-DHCR24 (Wuhan Aibotaike Biotechnology Co. Ltd.; cat. no. A5402) antibodies at a ratio of 1:250 (~0.2 μl of each antibody). The Duolink® Blocking Solution was removed by suction, and the diluted antibodies were evenly added to each slide. The slides were incubated at room temperature for 1 h or 4˚C overnight. PLUS and MINUS PLA probes (Sigma-Aldrich; Merck KGaA) were then vortexed and added to the Duolink® Antibody Diluent at a ratio of 1:5. The primary antibodies were removed by aspiration, washed with PBS for 2x5 min, and incubated with PLA solution for 1 h at 37˚C. The 5x Amplification buffer was then diluted into 1x Amplification buffer with sterile water and mixed well. The PLA solution was subsequently removed by aspiration and washed with PBS for 2x5 min. During this period, polymerase was added to the 1x Amplification buffer at a dilution of 1:80 to form an amplification reaction solution and mixed. The amplification reaction solution was added to the slide and incubated at 37˚C for 100 min. The amplification reaction solution was then removed by suction and washed with PBS for 3x10 min. A drop of Duolink® *In Situ* Mounting Medium with DAPI (Sigma-Aldrich; Merck KGaA) was then added onto the slide and the slide was transferred from the wet box to the slide. After 15 min, the cells were observed with a fluorescence microscope at a minimum magnification of x20. After the observation, the carrier plate was placed in the refrigerator at -20˚C.

Filipin staining. 5637 cells with good growth status were seeded into six-well plates at $5x10^6$ cells/well and cultured in a constant temperature incubator at 37˚C and 5% CO_2.When the cells reached ~50% confluency, the old medium was discarded and the cells were starved overnight. Drug treatment was added as aforementioned, and after 48 h of incubation, the old medium was removed by aspiration and washed three times by addition of PBS. After aspiration, the cells were fixed with 4% paraformaldehyde for 30 min at room temperature. The paraformaldehyde was then removed by aspiration and the cells were washed three times with PBS, stained with 1 ml PI added to each well, and incubated for 30 min at room temperature. PI staining was removed by aspiration and the cells were washed 3 times with PBS, treated with 1 ml glycine solution (1.5 mg/ml) per well for 10 min at room temperature, and washed 3 times with PBS at the end of treatment. PBS was removed by aspiration and 1 ml filipin staining solution (5 mg/ml) was added to each well at room temperature and they were left in the dark for 2 h. Filipin reagent was removed by suction and the cells were eluted 3 times with PBS. A drop of anti-fluorescence quenching solution was placed on the slide, a climbing slide was covered, the slides were sealed and labeled, and the slides were observed using fluorescence microscopy.

Statistical analysis. For bioinformatics analysis, the differential expression analysis of DHCR24 in the normal and cancer groups was performed using the unpaired t-test using the R language. The paired t-test was used for the paired analysis of differential expression of DHCR24 in cancer and adjacent tissues. The cell experiments were repeated three times for each group. In the filipin staining assays, differences between the two cell groups (control and EGF groups) were compared using an unpaired t-test. Differences between ≥3 groups were analyzed using one-way ANOVA followed by Tukey's post hoc test. Data are presented as mean ± standard deviation. $P<0.05$ was considered to indicate a statistically significant different. Statistical analysis was performed using GraphPad Prism 9.3 (Dotmatics).

Results

Pan-cancer analysis of DHCR24 expression. DHCR24 expression was first assessed across several cancers in the TCGA pan-cancer dataset. The findings revealed that DHCR24 exhibited differential expression across 12 cancer types (Fig. 1). Specifically, DHCR24 was significantly upregulated in seven cancers, including BLCA, BRCA, cervical cancer, liver cancer, prostate cancer, endometrial cancer and stomach cancer, whereas its expression was notably lower in glioblastoma, kidney chromophobe carcinoma, kidney renal clear cell carcinoma, lung squamous cell carcinoma (LUSC) and lung adenocarcinoma (Fig. 2A). To further assess these findings, the DHCR24 expression differences between tumor tissues and adjacent normal tissues were analyzed for these 12 cancers. The results demonstrated that, compared with in normal tissues, DHCR24 was significantly upregulated in BLCA, BRCA, liver cancer and prostate cancer tumor tissues, whilst it was downregulated in kidney chromophobe carcinoma, kidney renal clear cell carcinoma, lung adenocarcinoma and LUSC tumor tissues (Fig. 2B). These findings suggest that DHCR24 may serve distinct roles in different cancer types.

Prognostic and staging implications of DHCR24. To evaluate the prognostic relevance of DHCR24 in patients with cancer, a Kaplan-Meier OS analysis was performed, which revealed that high DHCR24 expression was significantly associated with a worse prognosis in BLCA compared with a low expression of DHCR24 (Fig. 3A). Furthermore, DFS analysis indicated that elevated DHCR24 expression was significantly associated with a worse prognosis in BRCA compared with a low expression of DHCR24 (Fig. 3B). Subsequently, DHCR24 expression across different cancer stages was further assessed using the World Health Organization staging system (20). The results demonstrated that DHCR24 expression increased with advancing cancer stages of BLCA ($P=0.0371$; Fig. 4A), whereas the opposite trend was observed in LUSC ($P=0.0466$; Fig. 4A); however, no significant stage-related variations were noted

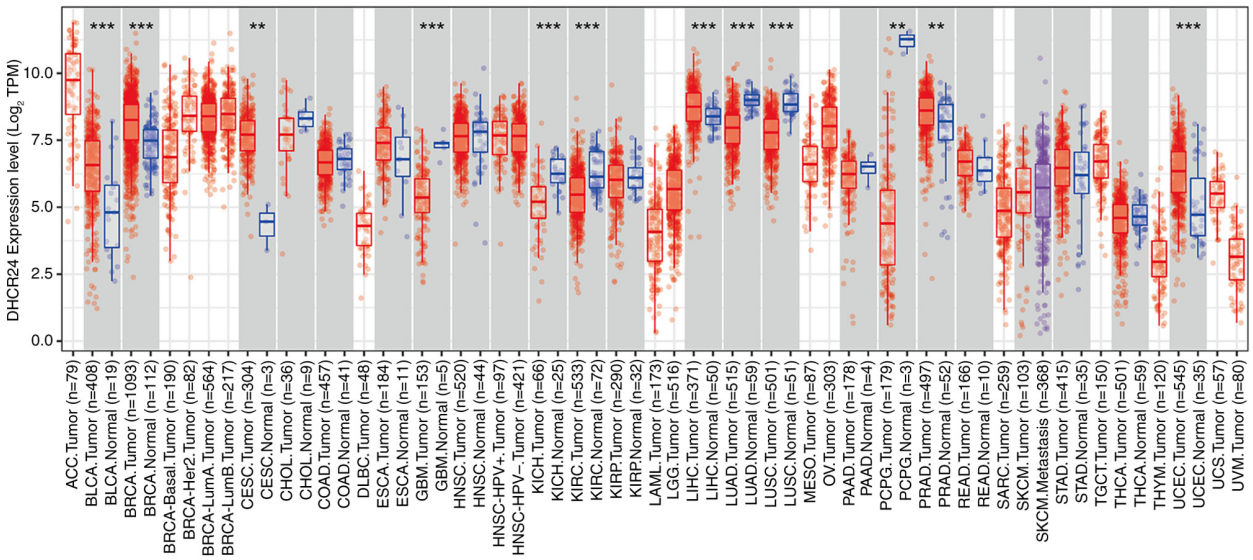

Figure 1. Upregulated mRNA expression of DHCR24 in pan-cancer. The results obtained from Tumor Immune Estimation Resource 2.0 were used for preliminary pan-cancer analysis of cancer data in The Cancer Genome Atlas, and they revealed that DHCR24 expression was significantly increased in 12 tumors compared with that in normal tissue. The red and blue boxes represent tumor tissues and normal tissues, respectively. **P<0.01; ***P<0.001. DHCR24, 3β-hydroxysteroid Δ24-reductase; TPM, transcripts per million. BLCA, bladder cancer; BRCA, breast invasive carcinoma; CESC, cervical squamous cell carcinoma and endocervical adenocarcinoma; GBM, glioblastoma multiforme; KICH, kidney chromophobe; KIRC, kidney renal clear cell carcinoma; LIHC, liver hepatocellular carcinoma; LUAD, lung adenocarcinoma; LUSC, lung squamous cell carcinoma; PRAD, prostate adenocarcinoma; UCEC, uterine corpus endometrial carcinoma; STAD, stomach adenocarcinoma.

in other cancers (Fig. 4A). Based on these findings, BLCA was prioritized for further functional analysis. A one-way Cox proportional hazards regression analysis was performed using TCGA data, which demonstrated that DHCR24 acts as an independent risk factor in BLCA (P=0.036; Fig. 4B). Additionally, multivariate Cox regression analysis confirmed that DHCR24 was an independent prognostic factor for BLCA (P=0.015; Fig. 4B), suggesting that DHCR24 expression significantly influences the survival of patients with BLCA. Moreover, ROC curve analysis further evaluated the prognostic use of DHCR24. The risk scores effectively stratified patients with BLCA based on prognosis at 1, 3 and 5 years (Fig. 4C). Notably, the predictive accuracy for 1-year survival was relatively high, with an area under the curve value of 0.575, whilst the predictive probability for survival beyond 1 year reached 0.725.

Biological characterization and consensus clustering analysis of differential genes. Given the pivotal role of DHCR24 in BLCA, a differential gene expression analysis was performed in BLCA using the limma package. Consensus clustering analysis (Fig. 5A) identified 11 hub genes closely associated with DHCR24, namely RAB7A, FAM83D, COMMD2, SLC9A3R1, IDI1, ECT2, AC078880.3, TESC, CRTAC1, RHEX and AL450384.2. A heatmap of differentially expressed genes in BLCA samples revealed a total of 2,958 differentially expressed genes (Fig. 5B). Pathway and enrichment analyses were performed using the clusterProfiler R package. GO enrichment analysis (Fig. 5C-E) revealed that these genes were primarily involved in extracellular matrix organization, collagen fibril organization and other processes critical to tumor microenvironment (TME) remodeling. They were predominantly associated with cellular components such as the collagen-containing extracellular matrix, collagen trimers and the endoplasmic reticulum lumen. Additionally, the molecular functions of these genes included extracellular matrix structural constituents, collagen binding and glycosaminoglycan binding. KEGG pathway enrichment analysis (Fig. 5F and G) identified key pathways enriched for these genes, including cytokine-cytokine receptor interactions, viral protein interactions with cytokine receptors, extracellular matrix (ECM)-receptor interactions, the calcium signaling pathway and the PI3K-Akt signaling pathway. Furthermore, gene set enrichment analysis revealed that DHCR24 expression was significantly associated with the chemokine signaling pathway, cytokine-cytokine receptor interactions and ECM-receptor interactions (Fig. 5H).

Analysis of DHCR24 expression and immune cell infiltration. To assess the relationship between DHCR24 and tumor immunity (Fig. 6A and B), the correlation between DHCR24 expression and immune cell infiltration levels in BLCA using the TCGA dataset was analyzed. The findings indicated that DHCR24 expression in BLCA was positively correlated with follicular helper T cells, dendritic cells and CD8+ T cells, whereas it was negatively correlated with naïve B cells, regulatory T cells and γΔ T cells. Immune surveillance serves a crucial role in cancer prognosis, as tumors can evade the immune response by exploiting immune checkpoints (21). The analysis revealed that DHCR24 expression was positively correlated with multiple immune checkpoint markers, including tumor necrosis factor ligand superfamily (TNFSF)9, hepatitis A virus cellular receptor 2, indoleamine 2,3-dioxygenase 1, V-set domain containing T cell activation inhibitor 1, TNFRSF18, neuropilin 1, CD276, CD44 and CD86, whilst it was negatively correlated with TNFRSF14 (P<0.001; Fig. 6C). Furthermore, DHCR24 expression showed a significant positive correlation with tumor mutational burden (TMB) in

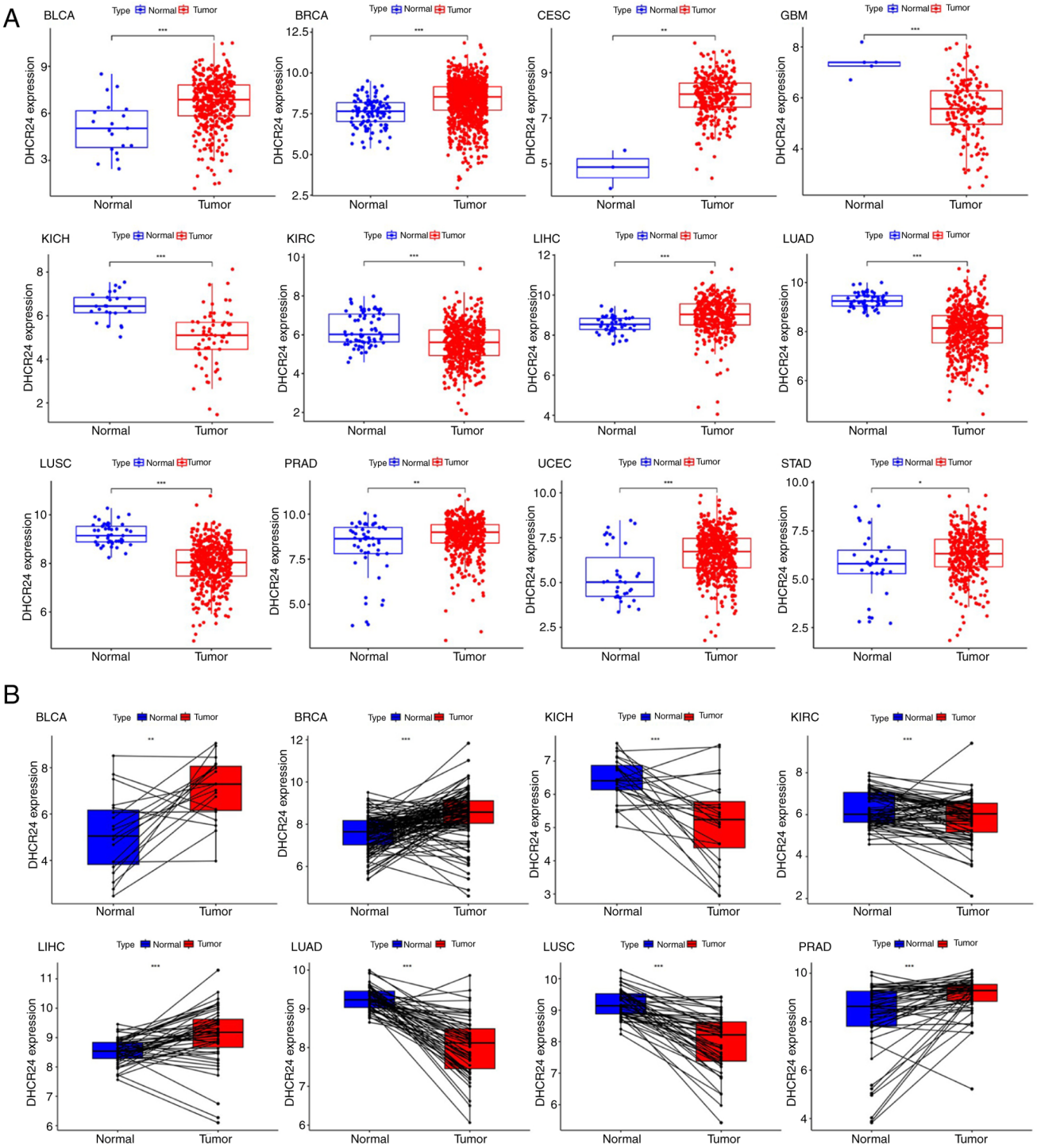

Figure 2. Expression of DHCR24 in different types of cancer. (A) Expression distribution of the DHCR24 gene in tumor and normal tissues. The differences between the two groups were compared. (B) Pan-cancer differential expression of DHCR24 in paired tumor and adjacent normal tissues in the indicated tumor types from The Cancer Genome Atlas database. *P<0.05, **P<0.01; ***P<0.001. DHCR24, 3β-hydroxysteroid Δ24-reductase; BLCA, bladder cancer; BRCA, breast invasive carcinoma; CESC, cervical squamous cell carcinoma and endocervical adenocarcinoma; GBM, glioblastoma multiforme; KICH, kidney chromophobe; KIRC, kidney renal clear cell carcinoma; LIHC, liver hepatocellular carcinoma; LUAD, lung adenocarcinoma; LUSC, lung squamous cell carcinoma; PRAD, prostate adenocarcinoma; UCEC, uterine corpus endometrial carcinoma; STAD, stomach adenocarcinoma.

BLCA (Fig. 6D), suggesting a potential role of DHCR24 in the tumor immune microenvironment.

DHCR24 expression in BLCA in the HPA database. To assess DHCR24 expression in BLCA, immunohistochemical images from the HPA database were analyzed. The results demonstrated that DHCR24 expression was markedly higher in BLCA tissues than in normal tissues (Fig. 7).

Establishment and analysis of the DHCR24 protein interaction database. Proteins rarely function in isolation; instead, they interact with other proteins to exert their biological

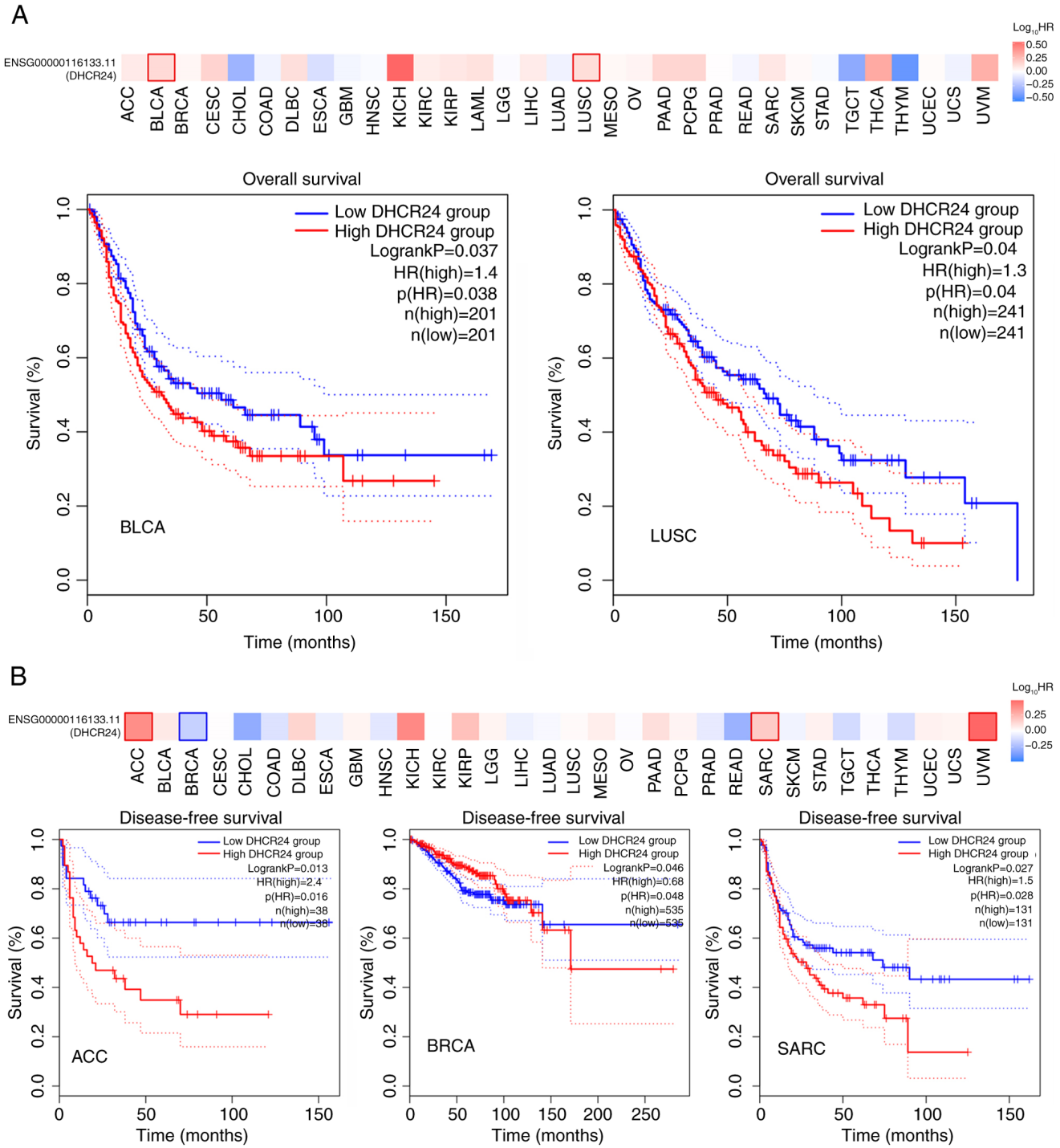

Figure 3. DHCR24 as a survival factor in some cancer types. The GEPIA2 tool was used to perform (A) overall survival and (B) disease-free survival analyses of different tumors in The Cancer Genome Atlas by DHCR24 gene expression. Survival maps and Kaplan-Meier curves with positive results are presented. DHCR24, 3β-hydroxysteroid Δ24-reductase; BLCA, bladder cancer; LUSC, lung squamous cell carcinoma; ACC, adrenocortical carcinoma; BRCA, breast cancer; SARC, sarcoma.

effects (22). To elucidate the functional role of DHCR24, a protein interaction analysis was performed to identify its potential interacting partners. IP-mass spectrometry using anti-DHCR24 antibodies and 293 cell lysates, combined with four publicly available protein interaction datasets, identified 492 proteins interacting with DHCR24 (unpublished data). Pathway enrichment analysis of this DHCR24 interaction network revealed significant enrichment in 20 signaling pathways, including the proteasome pathway, sterol biosynthesis pathway, viral oncogenic signaling pathway and endoplasmic reticulum protein processing pathway (Fig. 8A and B). These findings suggest that DHCR24 and its interacting proteins serve a critical role in sterol metabolism and cancer progression. To further assess the interaction network, a PPI network was constructed using STRING (Fig. 8C), with the dot size in the PPI network representing the contribution of each protein to network stability. Notably, DHCR24 exhibited a direct interaction with HRAS, as indicated by

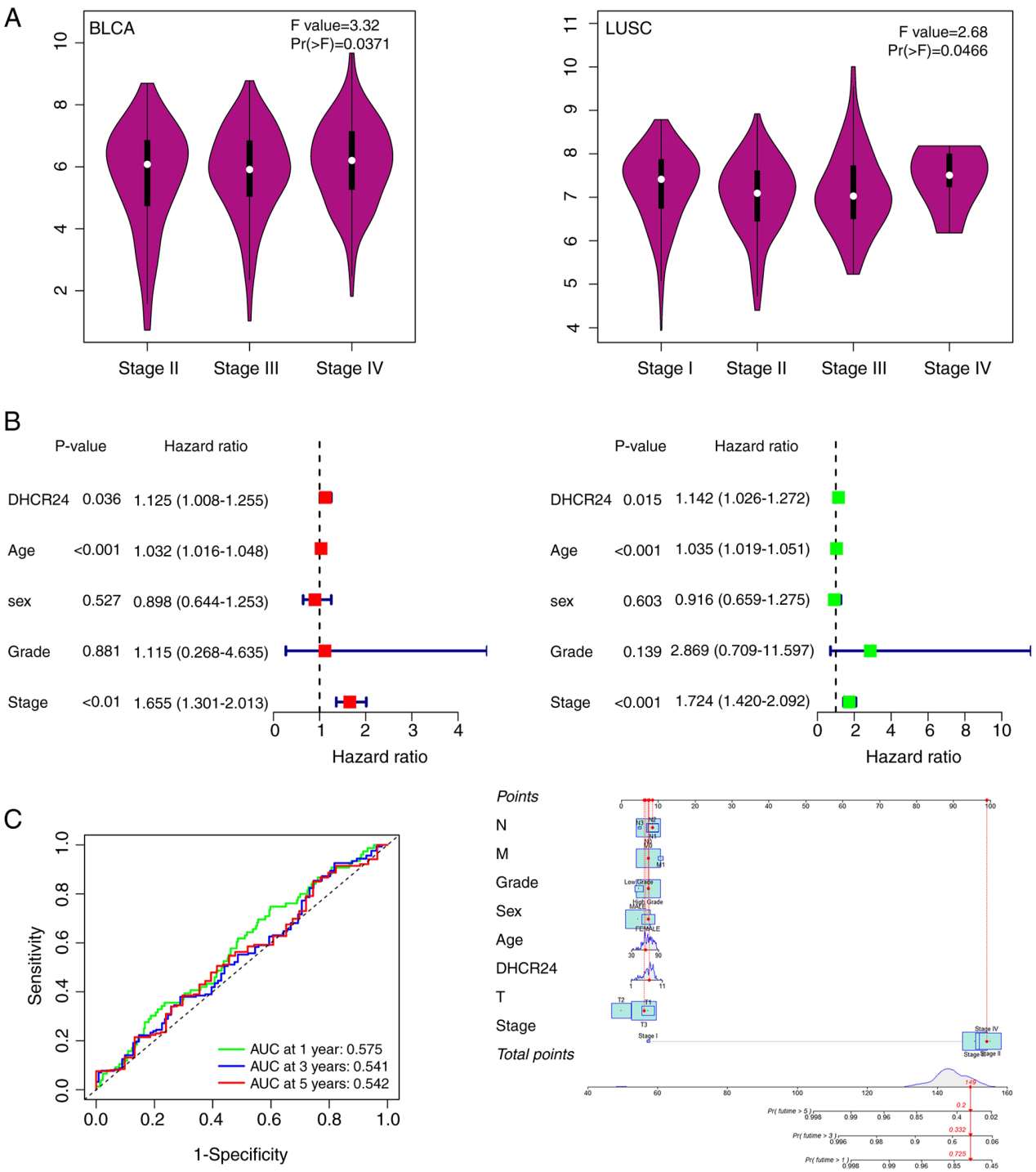

Figure 4. DHCR24 is a factor for clinical stage and the prognosis of cancer. (A) Based on The Cancer Genome Atlas data, the association between expression levels of the DHCR24 gene and the main pathological stages (stages I-IV) of BLCA and LUSC were analyzed. Log_2 (transcripts per million +1) was applied for log-scale. (B) Univariate and multifactorial proportional hazards model analyses. (C) Receiver operating characteristic curves demonstrated efficacy in predicting risk scores for the 1-, 3- and 5-year survival of patients, and the nomogram revealed the probability of predicting the 1-, 3- and 5-year survival of patients. DHCR24, 3β-hydroxysteroid Δ24-reductase; BLCA, bladder cancer; LUSC, lung squamous cell carcinoma; AUC, area under the curve; N, lymph node stage; M, metastasis stage; T, tumor stage.

a red dotted line between DHCR24 and HRAS. HRAS is a well-known oncogene that encodes a small GTPase involved in cancer progression (23). To further evaluate the functional significance of the DHCR24-HRAS interaction, DHCR24 and HRAS were chosen for the main nodes and a subnetwork was constructed consisting of all proteins directly interacting with them. Correlation analysis in the GEPIA database further demonstrated a positive correlation between DHCR24 and HRAS expression in cancer samples (Fig. 8D), highlighting their potential cooperative role in tumorigenesis.

Interaction between DHCR24 and HRAS. Using the Modeller sequence filtering function, all templates with ≥30% sequence homology to DHCR24 were selected for multitemplate

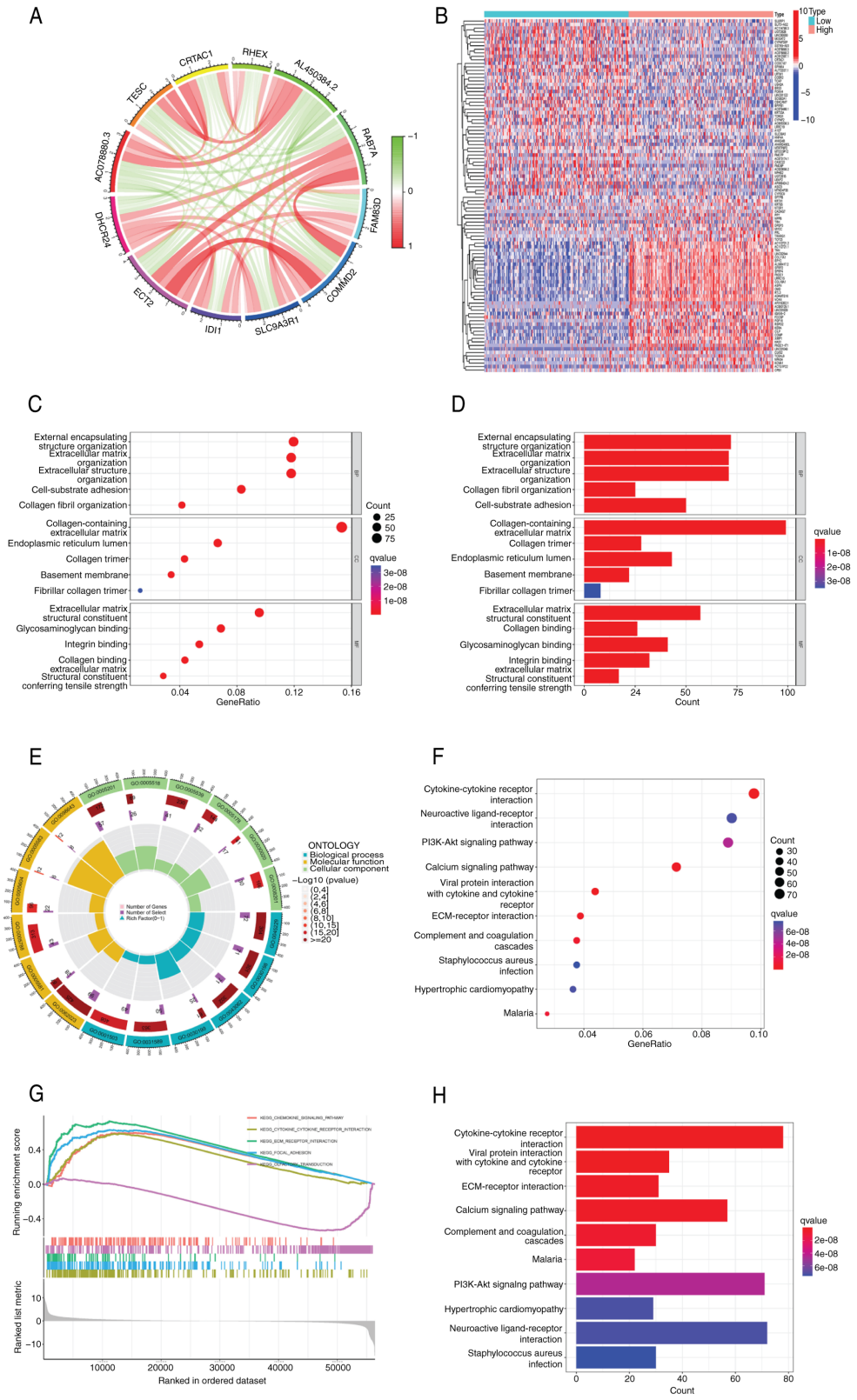

Figure 5. Important role of DHCR24 in bladder cancer. (A) Circos plot shows the correlation between the expression of several genes and DHCR24 in The Cancer Genome Atlas dataset. (B) Expression heat map of differential genes in bladder cancer. Gene Ontology analysis of the differently expressed genes was performed, and (C) bubble, (D) transverse bar and (E) circle charts were generated. KEGG analysis of the differently expressed genes was performed and (F) bubble and (G) transverse bar charts were generated. (H) Results of the Gene Set Enrichment Analysis of the differential genes. DHCR24, 3β-hydroxysteroid Δ24-reductase; KEGG, Kyoto Encyclopedia of Genes and Genomes.

modeling. The 3-dimensional (3D) model of DHCR24 was subsequently constructed using the Modeller multitemplate modeling function (Fig. 9A). Ramachandran plot analysis revealed that 86.6% of the residues fell within the most favorable region, 10.2% in the permissible region and only 3.3% in the outlier region. As an ideal 3D protein structure is expected

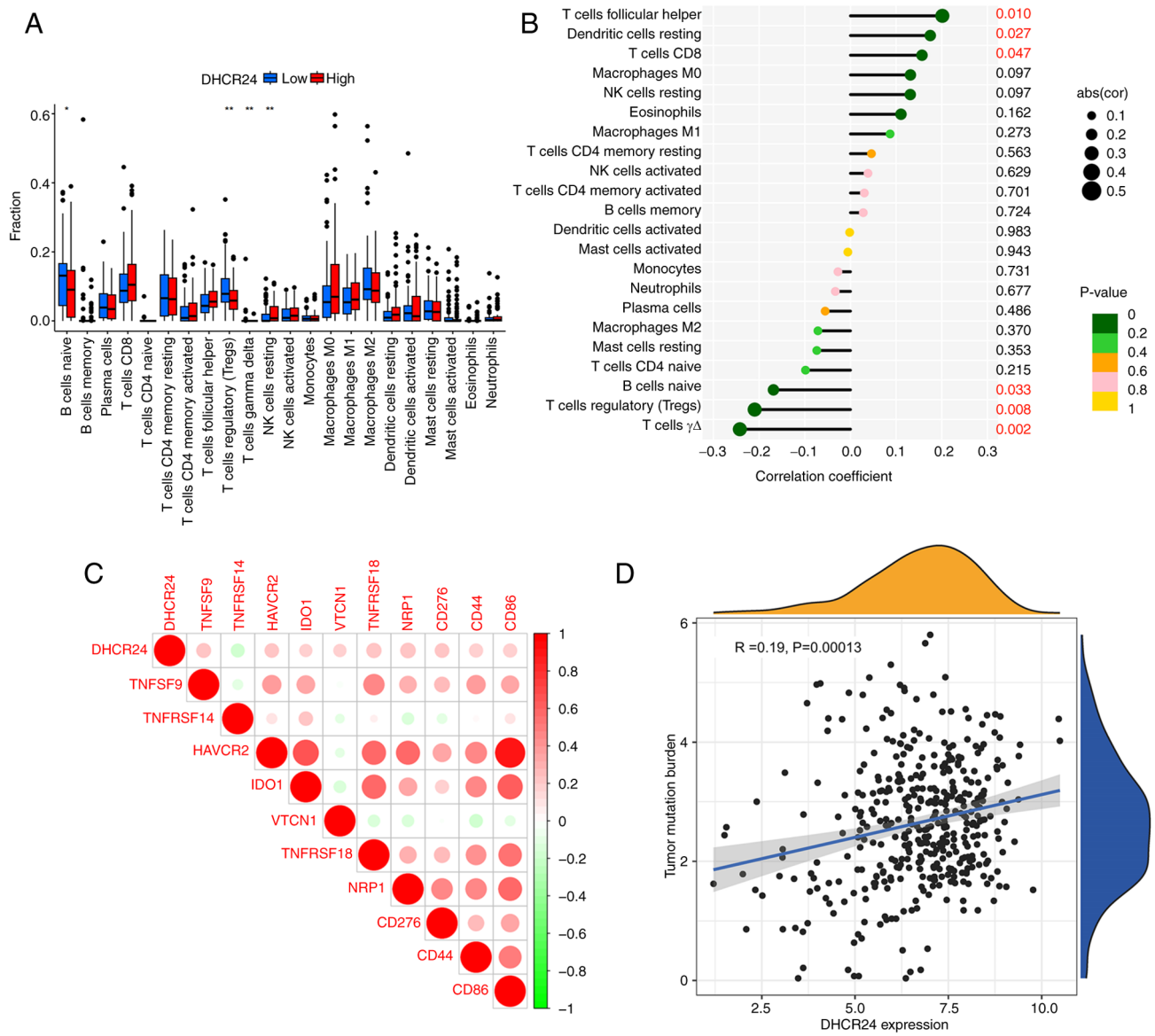

Figure 6. DHCR24 changes the tumor microenvironment of bladder cancer. (A) Differential analysis of immune cells in the DHCR24 low and high expression groups. Analysis of the correlation between DHCR24 expression and (B) immune cells and (C) tumor immune checkpoints. (D) Tumor mutation compliance analysis. *P<0.05, **P<0.01. DHCR24, 3β-hydroxysteroid Δ24-reductase; NK, natural killer.

to have ≥95% of its residues in the favorable and permissible regions (24), the results indicate that the modeled DHCR24 structure was high quality and well-suited for subsequent analyses (Fig. 9B).

HRAS interacts with the receptor-binding domain (RBD) region of PI3K, and EGF-mediated activation of HRAS leads to the activation of PI3K, thereby triggering downstream signaling pathways (25). To assess the molecular interaction between DHCR24 and HRAS, protein-protein docking was performed using the ZDOCK online server (Fig. 9C). A total of two docking strategies were used: Random docking and hotspot selection based on a DHCR24 homologous sequence similar to the RBD region of phosphatidylinositol-4,5-bisphosphate 3-kinase catalytic subunit γ. Notably, the top-ranked docking models generated by both strategies were nearly identical, as confirmed by Pymol-generated structural overlays (Fig. 9D) (26). These results suggest a direct and stable binding between DHCR24 and HRAS.

To further refine the binding mode between DHCR24 and HRAS, molecular dynamics simulations we performed using NAMD. The top-ranked conformation from ZDOCK docking was selected as the initial structure, and molecular dynamics simulations were performed to recalculate and optimize the docking results, providing a more accurate representation of the DHCR24-HRAS interaction (27). The root-mean-square deviation values for the DHCR24-HRAS binding system demonstrated an initial sharp increase within 15 nsec, followed by a gradual rise after 20 nsec and eventual stabilization after 55 nsec (Fig. 9E). Based on this, the stable complex conformation at 70 nsec was selected for interaction analysis (Fig. 9F) (28).

Using Pymol, the DHCR24-HRAS interaction interface was identified, which involved three structural regions of DHCR24: I45-K59, L354-P361 and Y440-R444. Notably, the L354-P361 region was homologous to the RBD domain of PI3K, whilst the L45-K59 region was located near the FAD-binding domain of

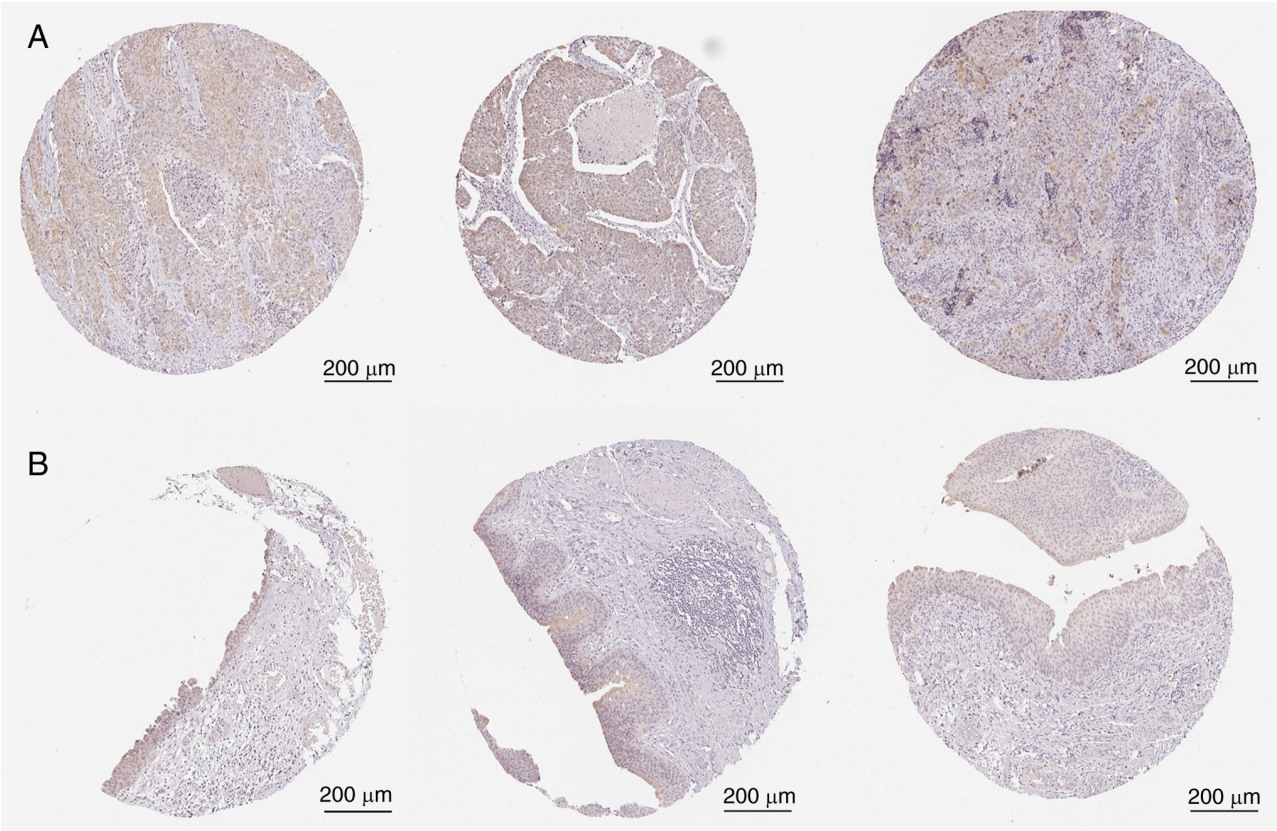

Figure 7. In the HPA database, DHCR24 is highly expressed in the immunohistochemical sections of bladder cancer. Immunohistochemical images of (A) cancerous bladder tissue from patients with bladder cancer and (B) normal human bladder tissue from the Human Protein Atlas database.

DHCR24. Subsequently, the interaction patterns of PI3K-HRAS (PDB: 1HE8) and DHCR24-HRAS were further compared using Pymol (Fig. 9G). The PI3K-HRAS interface in 1HE8 consisted of two complete α-helices and β-sheets, whereas the DHCR24-HRAS interface included two α-helices and two irregular loop regions, with one of the loops connecting to a β-sheet lamellar structure. These findings indicate a structural resemblance between the DHCR24-HRAS and PI3K-HRAS interaction models, suggesting that DHCR24 may functionally interact with HRAS in a manner similar to PI3K. Collectively, the aforementioned results provide strong evidence for a direct interaction between DHCR24 and HRAS, and this interaction may modulate DHCR24 activity via HRAS activation.

DHCR24 interacts with HRAS in vivo. To assess the interaction between DHCR24 and HRAS at the cellular level, 5637 cells, a human BLCA cell line with a naturally mutated HRAS, were used and the Duolink technique was applied for verification. The Duolink experiment results revealed scattered red fluorescent dots outside the nucleus in untreated 5637 cells (Normal group), indicating a direct interaction between DHCR24 and HRAS (Fig. 9H). Upon EGF stimulation (EGF group), a marked increase in the number of red fluorescent dots was observed compared with the Normal group, strongly suggesting that EGF enhances the interaction between DHCR24 and HRAS in 5637 cancer cells.

Role of DHCR24-HRAS interaction in bladder carcinogenesis. To evaluate the role of the DHCR24-HRAS interaction in bladder carcinogenesis, the present study assessed whether this interaction influences cancer cell proliferation by catalyzing cholesterol synthesis. 5637 cells were treated with EGF, lonafarnib (an HRAS inhibitor) and U18666A (a DHCR24 inhibitor) in different combinations and cell proliferation was assessed. In the absence of EGF stimulation, similar numbers of adherent cells were observed across all groups. However, in the U18666A-treated group, the number of adherent cells was notably reduced compared with the normal group, indicating that U18666A inhibited 5637 cell proliferation (Fig. 10A). Furthermore, Compared with that in the untreated control group, the number of adherent cells in the EGF group was significantly increased, demonstrating that EGF promotes 5637 cell proliferation. Notably, the addition of U18666A to EGF-stimulated cells (EGF + U18666A group) led to a marked reduction in adherent cells compared with the EGF-only group, indicating that U18666A blocked EGF-induced proliferation. Similarly, the EGF + lonafarnib group also demonstrated a notable decrease in adherent cells compared with the EGF group, suggesting that lonafarnib-mediated HRAS inhibition suppressed EGF-induced cell proliferation. These findings align with that of previous studies (29,30). In addition, cell adhesion assessment has certain limitations, for example, adherent cells do not directly represent the potential of cell proliferation. In addition, only cells with both adherent and proliferative activities can form cell clones, which can better reflect cell life. So w the cell viability assay was performed. Evaluated cell proliferation was further using the MTT assay, which yielded results consistent with the aforementioned observations (Fig. 10B).

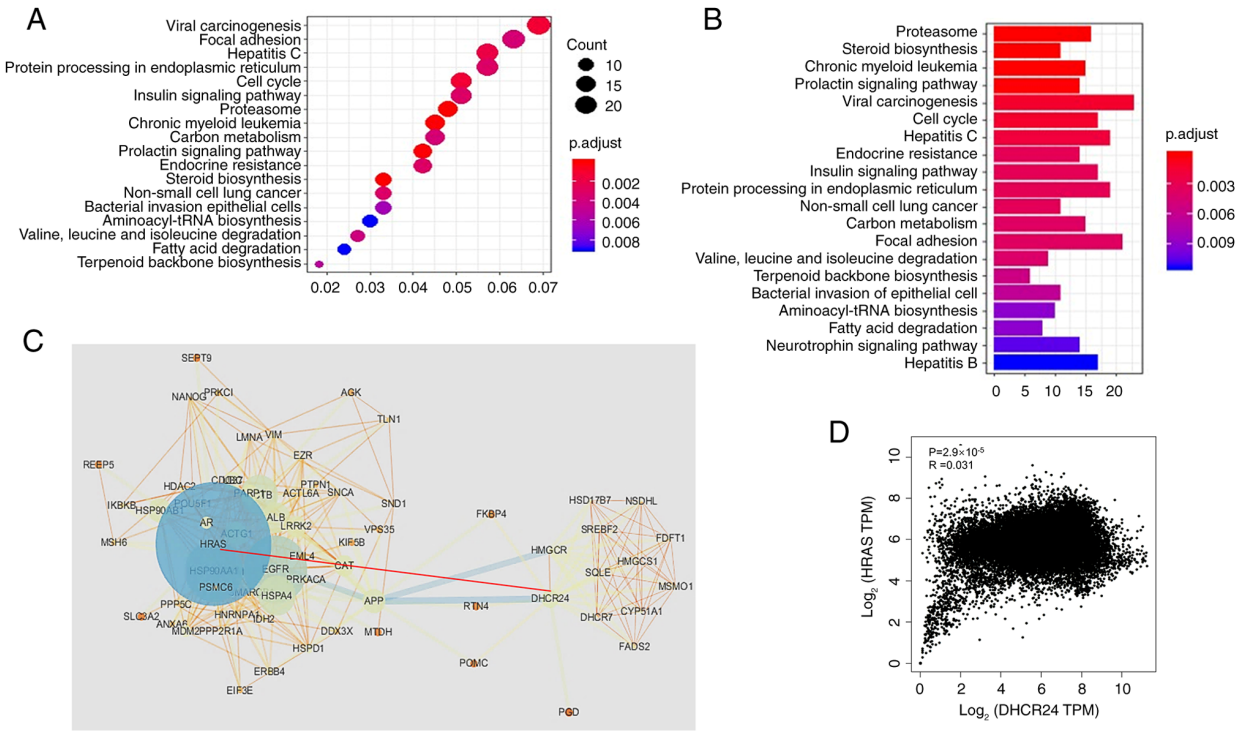

Figure 8. DHCR24 may interact with HRAS to play a role in cancer. (A) Bubble map and (B) histogram of the Kyoto Encyclopedia of Genes and Genomes analysis of the DHCR24-interacting proteome. (C) Protein-protein interaction network formed by DHCR24 and HRAS. (D) Correlation analysis of DHCR24 and HRAS expression in the GEPIA database. DHCR24, 3β-hydroxysteroid Δ24-reductase; tRNA, transfer RNA; TPM, transcripts per million.

To assess whether the EGF-driven proliferation of 5637 cells was associated with increased cholesterol synthesis, fluorescence staining was performed using the cholesterol-specific fluorescent dye, filipin. Fluorescence microscopy revealed that blue fluorescence intensity corresponded with intracellular cholesterol levels. Weak fluorescence was observed in untreated 5637 cells (Fig. 10C), whereas the EGF group showed significantly enhanced fluorescence on the cell membrane compared with the untreated control group, indicating increased cholesterol content (Fig. 10D).

To determine whether EGF-induced cholesterol synthesis is dependent on DHCR24 and HRAS, both untreated and EGF-stimulated cells were treated with lonafarnib and U18666A and the cholesterol content was assessed using filipin staining. U18666A, but not lonafarib, significantly reduced cholesterol synthesis in normal 5637 cells compared with the control (Fig. 10E), suggesting that cholesterol synthesis in unstimulated 5637 cells requires DHCR24 activity but is not primarily dependent on HRAS activation. However, in EGF-treated cells, both U18666A and lonafarnib significantly inhibited cholesterol synthesis compared with the EGF group (Fig. 10F), indicating that EGF-driven cholesterol synthesis relies on the interaction between HRAS and DHCR24.

Discussion

Cancer remains a significant threat to human health due to its high morbidity and mortality rates, which have been rising in recent years (31). Cancer treatments are broadly classified into chemotherapy, radiotherapy and surgery; however, many patients lack access to these treatments. For instance, patients with advanced metastases rarely qualify for surgical resection, whilst certain individuals are unable to tolerate the severe side effects of chemotherapy and radiotherapy. Additionally, targeted therapy is only suitable for a limited subset of patients. Certain genetically predisposed cancers, such as CRC, pose particular challenges in achieving optimal prognostic outcomes through tailored drug therapies (32). Therefore, early detection and timely intervention are critical for improving cancer prognosis (33). Given the heterogeneity of cancer, treatment strategies are often individualized, with personalized therapy becoming increasingly prevalent (34). Pan-cancer analyses offer valuable insights into the commonalities and differences among several cancers, providing a foundation for personalized treatment approaches (35). Moreover, this type of analysis helps elucidate the relationship between genetic mutations and cancer progression, and, as research advances, it may serve a pivotal role in promoting early cancer diagnosis and treatment (36,37).

DHCR24, the terminal enzyme in cholesterol biosynthesis, is closely associated with several diseases, particularly hyperlipidemia and hypercholesterolemia, which are major risk factors for cardiovascular diseases such as atherosclerosis, coronary artery disease and ischemic heart disease (38). The liver, a key organ in fat metabolism, has been reported to be markedly impacted by DHCR24 activity. Research indicates that suppression of DHCR24 expression can prevent diet-induced hepatic steatosis and inflammation in an Liver X receptor α-dependent manner (39). Furthermore, hypercholesterolemia has been strongly associated with the development of steroid hormone-regulated cancers, including breast and prostate cancer (40,41). A previous study also suggested a

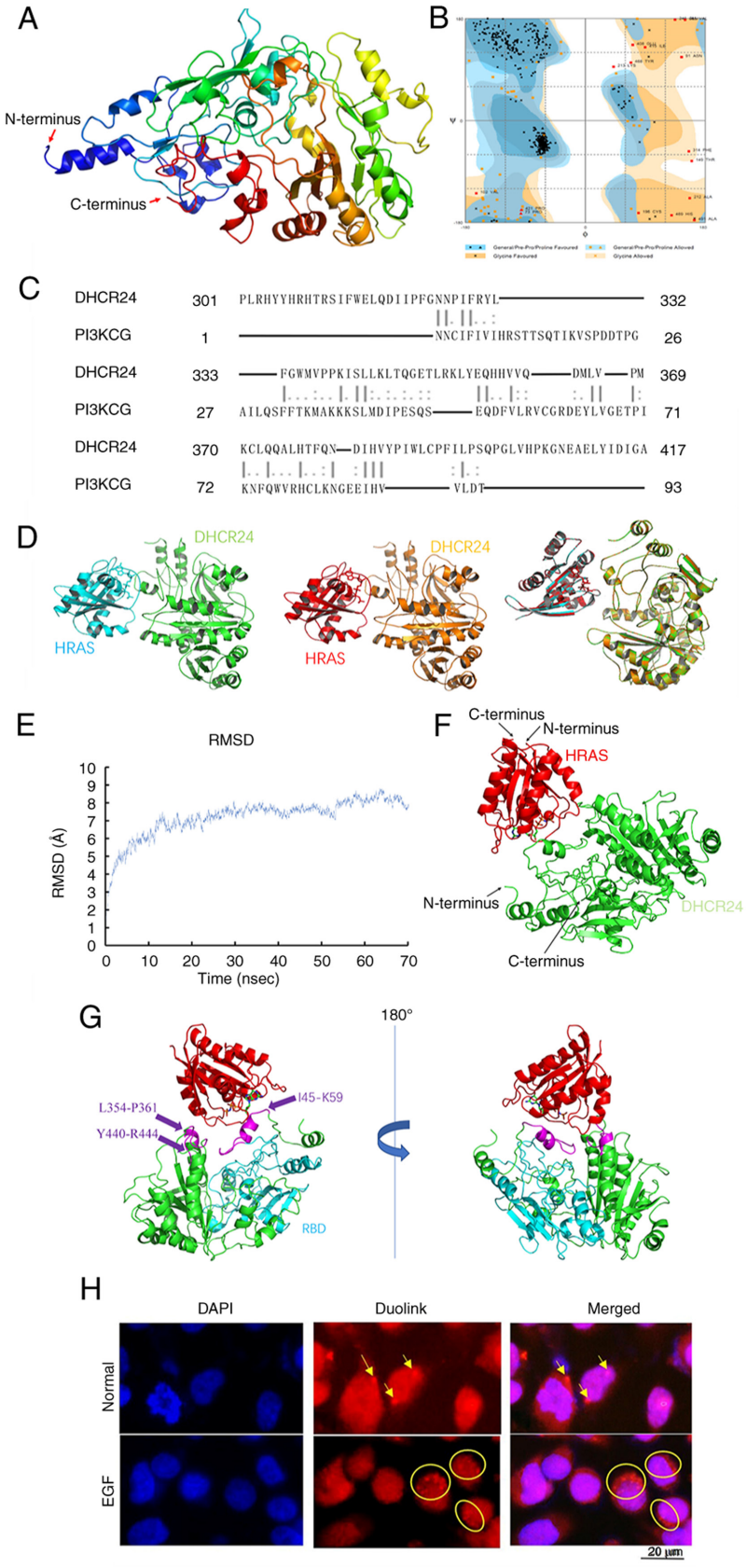

Figure 9. DHCR24 interacts with HRAS *in vivo*. (A) Modeller multi-template modeling of the constructed DHCR24 structure. (B) Pulled graph analysis of DHCR24 with multiple template modeling. (C) Sequence alignment between the receptor-binding domain region of PI3KCG and DHCR24. (D) ZDOCK results show that DHCR24 and HRAS are able to interact with each other. Random docking results: Blue for HRAS and green for DHCR24; hot spot docking results: Red for HRAS and orange for DHCR24; both comparison results. (E) Trunk plot of RMSD vs. time for DHCR24 in complex with HRAS. (F) Stable three-dimensional structure of DHCR24 complexed with HRAS after 70 nsec of kinetic simulation. (G) Stable three-dimensional structure of DHCR24 complexed with HRAS after 70 nsec of kinetic simulation. (H) 5637 cells were stained with Duolink using mouse-derived anti-HRAS with rabbit-derived anti-DHCR24 and their nuclei were stained with DAPI. Images were captured using fluorescence microscopy. DHCR24, 3β-hydroxysteroid Δ24-reductase; RMSD, root mean square deviation; PI3KCG, phosphatidylinositol-4,5-bisphosphate 3-kinase catalytic subunit γ.

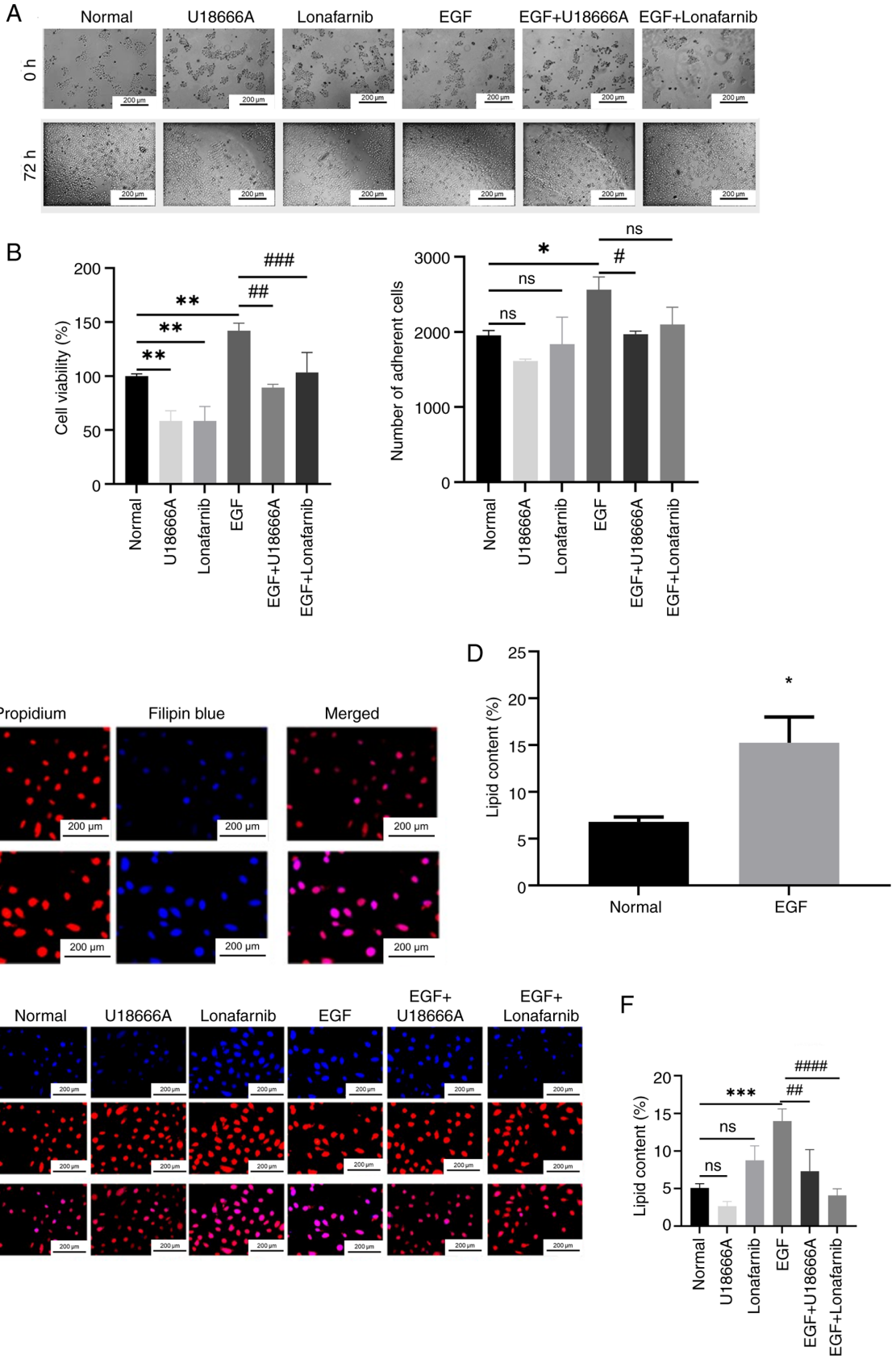

Figure 10. Role of DHCR24-HRAS interaction in bladder carcinogenesis. (A) 5637 cells were stimulated with several drugs, and cell proliferation was observed after 72 h using light microscopy and cell counting. normal: 5637 cells cultured in normal medium without drug stimulation; U18666A: 5637 cells in normal culture with U18666A added; lonafarnib: 5637 cells in normal culture with lonafarnib added; EGF: 5637 cells in normal culture with the addition of EGF; EGF + U18666A: 5637 cells in normal culture with the addition of both EGF and U18666A; and EGF + Lonafarnib: 5637 cells in normal culture with the addition of both EGF and lonafarnib. (B) Cell proliferation measured by MTT assay (left) and number of adherent cells at 72 h (right). (C) Fluorescence staining of Filipin in 5637 cells after EGF stimulation. (D) Analysis of filipin fluorescence intensity of 5637 cells with (EGF group) and without (Normal group) EGF stimulation. (E) Fluorescence staining of Filipin in 5637 cells after the administration of U18666A and lonafarnib. (F) Filipin fluorescence intensity analysis. *P<0.05; **P<0.01; ***P<0.001 normal vs. negative control group; $^{\#}$P<0.05; $^{\#\#}$P<0.01; $^{\#\#\#}$P<0.001; $^{\#\#\#\#}$P<0.001 EGF vs. experimental group. EGF, epidermal growth factor; ns, not significant.

link between hypercholesterolemia and BLCA, although the underlying mechanisms remain unclear (42).

Through a pan-cancer analysis of DHCR24, the present study demonstrated aberrant DHCR24 expression across multiple cancer types, and identifying it as an independent prognostic factor for BLCA. This suggests that DHCR24 may serve as a biomarker for early BLCA diagnosis and treatment. Enrichment analysis of DHCR24-associated differentially expressed genes in BLCA also revealed strong associations with cytokines and their receptors, viral infections and the PI3K-Akt signaling pathway. Viral infections are well-documented oncogenic factors; for example, Epstein-Barr virus has been implicated in BRCA and gastric cancer (43,44). The PI3K-Akt signaling pathway, a key regulator of cell survival, is widely recognized as a major driver of cancer progression and therapeutic resistance (45), Notably, numerous studies have highlighted the notable role of PI3K-Akt pathway activation in the development of urological malignancies (46,47).

TME, immune checkpoints and TMB are key areas of focus in cancer research. Growing evidence indicates that interactions between cancer cells and several components of the TME contribute to immune evasion, ultimately promoting tumor proliferation, recurrence and metastasis (48). Immune checkpoints and TMB partially influence treatment strategies for patients with cancer (49). In the present study, in BLCA, DHCR24 expression was positively correlated with T-cell follicular helper cells, dendritic cells and CD8+ T cells, whereas it was negatively correlated with naïve B cells, regulatory T cells and γδ T cells. This suggests that DHCR24 is also involved in the metastatic progression of BLCA.

RAS proteins are the founding members of the RAS superfamily of small GTPases and are central to a highly complex signaling network that regulates key cellular processes, including differentiation, survival and proliferation (50). These proteins serve a crucial role in tumorigenesis, with point mutations leading to chronic RAS activation in ~30% of human tumors (51). RAS proteins are typically activated by guanine nucleotide exchange factors, such as Son of sevenless homolog 1, and inactivated by GTPase-activating proteins (52). In cancer, RAS activation is enhanced through multiple mechanisms, including amplification of signals from oncogenic or wild-type RAS, increased upstream inputs such as receptor tyrosine kinases or guanine nucleotide exchange factors (51), or the loss of negative regulators such as GTPase-activating proteins or Sprouty related EVH1 domain/Sprouty-mediated feedback inhibition (53). The TCGA project identified RTK-RAS signaling as the most frequently altered oncogenic pathway, occurring in ~46% of cancer samples. RAS mutations are implicated in 20-30% of human cancers, with KRAS mutations predominantly found in pancreatic and CRCs, whereas NRAS mutations are more frequent in melanoma, thyroid cancer and leukemia (54-57). Although KRAS, NRAS and HRAS share similar functions, KRAS mutations typically occur at codon 12, whilst HRAS and NRAS mutations are more commonly observed at codon 61 (58). These mutations disrupt the regulatory mechanisms of RAS signaling, leading to sustained pro-proliferative signaling downstream of growth factor receptors (58,59).

In a previous study, when DHCR24 was knocked down in HepG2 cells cultured in the presence of fetal bovine serum, normal cell proliferation was maintained. However, under fat-free serum conditions, DHCR24 knockdown markedly reduced cell viability after 48 h, suggesting that desmosterol cannot fully compensate for cholesterol, at least in terms of supporting cell proliferation (60). By contrast, other studies suggest that desmosterol can displace cholesterol in cellular membranes (61). Although the functional equivalence of desmosterol and cholesterol in the plasma membrane remains debated, their effects appear to differ depending on the tumor cell type. Our previous study using DHCR24 knockout (DHCR24-/-) mouse embryonic fibroblasts demonstrated that while desmosterol accumulated in these cells, its levels remained notably lower than cholesterol levels in wild-type cells. This suggests that the downregulation of DHCR24 exerts a broader inhibitory effect on the cholesterol synthesis pathway (62). Thus, in certain tumor cells, reduced DHCR24 expression not only leads to decreased cholesterol levels but also results in a comparatively lower desmosterol concentration than in cells with normal DHCR24 expression. Additionally, our previous study demonstrated that DHCR24 functions as a hydrogen peroxide scavenger, protecting cells from oxidative stress-induced apoptosis (63). Moreover, DHCR24-mediated sterol homeostasis is essential for mitochondrial sheath formation during spermatogenesis, highlighting its critical role in both the urinary and reproductive systems (64). These findings suggest that abnormal DHCR24 expression in different cancer cells contributes to tumorigenesis through diverse mechanisms beyond desmosterol accumulation alone.

The androgen receptor-mediated PI3K/Akt signaling pathway has been reported to regulate DHCR24 expression. Additionally, DHCR24 has been implicated in the development of human BLCA (65). This suggests that DHCR24 overexpression is associated with BLCA pathogenesis in males. Notably, studies have reported that a diet high in selenium or isoflavones can markedly regulate DHCR24 enzyme activity downstream of the androgen receptor, indicating that such dietary habits may provide protective effects against the development of hormone-related cancers (66,67).

Through molecular docking, kinetic simulations and Duolink experiments, the present study demonstrated that DHCR24 interacts with HRAS and that HRAS activation may influence DHCR24 activity, thereby affecting its ability to synthesize cholesterol. Furthermore, experiments using EGF, lonafarnib and U18666A (alone or in combination) in BLCA 5637 cells revealed that the HRAS-DHCR24 interaction enhances cholesterol synthesis, ultimately promoting cell proliferation in BLCA.

DHCR24 is an enzyme involved in the final step of cholesterol synthesis and exhibits notable variation in cholesterol content in BLCA cells (68); however, a limitation of the present study is the use of a single human BLCA cell line. In related BLCA research, other commonly used cell lines, such as T24, RT4 and J82, are also frequently employed (69). Further study of gene function usually involves gene knockdown or deletion. The preset study also has certain limitations in this respect. In the follow-up study, a BLCA DHCR24 knockout cell line can be created to further explore the relationship between DHCR24 and the occurrence and development time of BLCA. Therefore, future research should verify the findings

of the present study across several BLCA cell lines, which will be valuable for the classification and precision treatment of BLCA. Moreover, it is currently unclear as to whether there are differences in cholesterol content in other parts of the body, and this should be addressed through subsequent animal experiments in BLCA xenograft mice.

In summary, the results of the present study demonstrated that DHCR24 is highly expressed in BLCA and serves as an independent prognostic factor, with significant implications for tumor progression and treatment strategies. Through pan-cancer analysis, its association with the TME, TMB and immune cell infiltration was established, suggesting its potential role in tumorigenesis and metastasis. Further molecular docking, dynamic simulations and cellular experiments revealed that DHCR24 interacts with HRAS, enhancing cholesterol synthesis and promoting BLCA cell proliferation. The effects of EGF, lonafarnib and U18666A on 5637 cells further demonstrated the role of DHCR24-HRAS interaction in tumor growth. Given its involvement in key oncogenic pathways, DHCR24 may serve as a biomarker for BLCA prognosis and a potential therapeutic target. Future prospective studies and animal experiments are warranted to explore the role of DHCR24 in immune cell infiltration and its potential impact on immunotherapy efficacy, paving the way for personalized treatment strategies targeting DHCR24 in BLCA.

Acknowledgements

Not applicable.

Funding

This research was funded by grants from the National Natural Science Foundation of China (nos. 82070722, 82300865 and 82470798).

Availability of data and materials

The data generated in the present study may be requested from the corresponding author.

Authors' contributions

ZW, XL and BG conceptualized the study, designed the methodology and interpreted data. JM and ZL conducted cell experiments. ZW and YZ performed data acquisition. WY and YZ conducted the statistical analyses. YZ participated in the drafting of the manuscript and critical revisions for important intellectual content and images. BG and DS participated in the study design. XL and BG confirm the authenticity of all the raw data. All authors have read and approved the final manuscript.

Ethics approval and consent to participate

Not applicable.

Patient consent for publication

Not applicable.

Competing interests

The authors declare that they have no competing interests.

References

1. Haas MJ and Mooradian AD: Potential therapeutic agents that target ATP binding cassette A1 (ABCA1) gene expression. Drugs 82: 1055-1075, 2022.
2. Wahida A, Buschhorn L, Fröhling S, Jost PJ, Schneeweiss A, Lichter P and Kurzrock R: The coming decade in precision oncology: Six riddles. Nat Rev Cancer 23: 43-54, 2023.
3. Zhou C, Solomon B, Loong HH, Park K, Pérol M, Arriola E, Novello S, Han B, Zhou J, Ardizzoni A, *et al*: First-line selpercatinib or chemotherapy and pembrolizumab in RET Fusion-positive NSCLC. N Engl J Med 389: 1839-1850, 2023.
4. Last AR, Ference JD and Menzel ER: Hyperlipidemia: Drugs for cardiovascular risk reduction in adults. Am Fam Physician 95: 78-87, 2017.
5. Nong S, Han X, Xiang Y, Qian Y, Wei Y, Zhang T, Tian K, Shen K, Yang J and Ma X: Metabolic reprogramming in cancer: Mechanisms and therapeutics. MedComm (2020) 4: e218, 2023.
6. Giacomini I, Gianfanti F, Desbats MA, Orso G, Berretta M, Prayer-Galetti T, Ragazzi E and Cocetta V: Cholesterol metabolic reprogramming in cancer and its pharmacological modulation as therapeutic strategy. Front Oncol 11: 682911, 2021.
7. Patel K and Kashfi K: Lipoproteins and cancer: The role of HDL-C, LDL-C, and cholesterol-lowering drugs. Biochem Pharmacol 196: 114654, 2022.
8. Pelton K, Freeman M and Solomon K: Cholesterol and prostate cancer. Curr Opin Pharmacol 12: 751-759, 2012.
9. Jun SY, Brown AJ, Chua NK, Yoon JY, Lee JJ, Yang JO, Jang I, Jeon SJ, Choi TI, Kim CH and Kim NS: Reduction of squalene epoxidase by cholesterol accumulation accelerates colorectal cancer progression and metastasis. Gastroenterology 160: 1194-1207.e28, 2021.
10. Baek AE, Yu YA, He S, Wardell SE, Chang CY, Kwon S, Pillai RV, McDowell HB, Thompson JW, Dubois LG, *et al*: The cholesterol metabolite 27 hydroxycholesterol facilitates breast cancer metastasis through its actions on immune cells. Nat Commun 8: 864, 2017.
11. Zhao Y, Chen J, Zheng H, Luo Y, An M, Lin Y, Pang M, Li Y, Kong Y, He W, *et al*: SUMOylation-Driven mRNA circularization enhances translation and promotes lymphatic metastasis of bladder cancer. Cancer Res 84: 434-448, 2023.
12. Luu W, Zerenturk EJ, Kristiana I, Bucknall MP, Sharpe LJ and Brown AJ: Signaling regulates activity of DHCR24, the final enzyme in cholesterol synthesis. J Lipid Res 55: 410-420, 2014.
13. Lu Z, Wang H, Zhang X, Huang X, Jiang S, Li Y, Liu T, Lu X and Gao B: High fat diet induces brain injury and neuronal apoptosis via down-regulating 3-β hydroxycholesterol 24 reductase (DHCR24). Cell Tissue Res 393: 471-487, 2023.
14. Chen CH, Weng TH, Huang KY, Kao HJ, Liao KW and Weng SL: Anticancer peptide Q7 suppresses the growth and migration of human endometrial cancer by inhibiting DHCR24 expression and modulating the AKT-mediated pathway. Int J Med Sci 19: 2008-2021, 2022.
15. Wu J, Guo L, Qiu X, Ren Y, Li F, Cui W and Song S: Genkwadaphnin inhibits growth and invasion in hepatocellular carcinoma by blocking DHCR24-mediated cholesterol biosynthesis and lipid rafts formation. Br J Cancer 123: 1673-1685, 2020.
16. Yuan W, Yong W, Zhu J and Shi D: DPP4 regulates DHCR24-mediated cholesterol biosynthesis to promote methotrexate resistance in gestational trophoblastic neoplastic cells. Front Oncol 11: 704024, 2021.
17. Yan-Long S, Ming-Bo L, Hong-Ting W, Ye H and Xuan H: GLTP is a potential prognostic biomarker and correlates with immunotherapy efficacy in cervical cancer. Dis Markers 2022: 9109365, 2022.
18. Zeynab A, Nasrin Z and Roghayeh A: Anticancer effects of cinnamaldehyde through inhibition of ErbB2/HSF1/LDHA pathway in 5637 cell line of bladder cancer. Anticancer Agents Med Chem 22: 1139-1148, 2022.
19. Motie FM, Soltani Howyzeh M and Ghanbariasad A: Synergic effects of DL-limonene, R-limonene, and cisplatin on AKT, PI3K, and mTOR gene expression in MDA-MB-231 and 5637 cell lines. Int J Biol Macromol 280: 136216, 2024.

20. Pezeshki S, Hashemi P, Salimi A, Ebrahimi S, Javanzad M and Monfaredan A: Evaluation of NUF2 and GMNN expression in prostate cancer: Potential biomarkers for prostate cancer screening. Rep Biochem Mol Biol 10: 224-232, 2021.
21. Xia L, Oyang L, Lin J, Tan S, Han Y, Wu N, Yi P, Tang L, Pan Q, Rao S, *et al*: The cancer metabolic reprogramming and immune response. Mol Cancer 20: 28, 2021.
22. Gonzalez MW and Kann MG: Chapter 4: Protein interactions and disease. PLoS Comput Biol 8: e1002819, 2012.
23. Astrain G, Nikolova M and Smith MJ: Functional diversity in the RAS subfamily of small GTPases. Biochem Soc Trans 50: 921-933, 2022.
24. Jumper J, Evans R, Pritzel A, Green T, Figurnov M, Ronneberger O, Tunyasuvunakool K, Bates R, Žídek A, Potapenko A, *et al*: Highly accurate protein structure prediction with AlphaFold. Naturev 596: 583-589, 2021.
25. Wee P and Wang Z: Epidermal growth factor receptor cell proliferation signaling pathways. Cancers (Basel) 9: 52, 2017.
26. Delano WL: The PyMol molecular graphics system. Proteins Structure Function Bioinformatics 30: 442-454, 2002.
27. Phillips JC, Braun R, Wang W, Gumbart J, Tajkhorshid E, Villa E, Chipot C, Skeel RD, Kalé L and Schulten K: Scalable molecular dynamics with NAMD. J Comput Chem 26: 1781-802, 2005.
28. Wang H, Lu Z, Li Y, Liu T, Zhao L, Gao T, Lu X and Gao B: Virtual screening of Novel 24-dehydroxysterol reductase (DHCR24) inhibitors and the biological evaluation of irbesartan in Cholesterol-lowering effect. Molecules 28: 2643, 2023.
29. Liu T, Li Y, Yang B, Wang H, Lu C, Chang AK, Huang X, Zhang X, Lu Z, Lu X and Gao B: Suppression of neuronal cholesterol biosynthesis impairs brain functions through insulin-like growth factor I-Akt signaling. Int J Biol Sci 17: 3702-3716, 2021.
30. Quan X, Chen X, Sun D, Xu B, Zhao L, Shi X, Liu H, Gao B and Lu X: The mechanism of the effect of U18666a on blocking the activity of 3β-hydroxysterol Δ-24-reductase (DHCR24): Molecular dynamics simulation study and free energy analysis. J Mol Model 22: 46, 2016.
31. Sung H, Ferlay J, Siegel RL, Laversanne M, Soerjomataram I, Jemal A and Bray F: Global cancer statistics 2020: GLOBOCAN estimates of incidence and mortality worldwide for 36 cancers in 185 countries. CA Cancer J Clin 71: 209-249, 2021.
32. Yang Y, Liu P, Zhou M, Yin L, Wang M, Liu T, Jiang X and Gao H: Small-molecule drugs of colorectal cancer: Current status and future directions. Biochim Biophys Acta Mol Basis Dis 1870: 166880, 2024.
33. Crosby D, Bhatia S, Brindle KM, Coussens LM, Dive C, Emberton M, Esener S, Fitzgerald RC, Gambhir SS and Kuhn P: Early detection of cancer. Science 375: eaay9040, 2022.
34. Zhang X, Xie J, Yang Z, Yu CKW, Hu Y and Qin J: Tumour heterogeneity and personalized treatment screening based on single-cell transcriptomics. Comput Struct Biotechnol J 27: 307-320, 2024.
35. Li J, Li X, Huang H, Tao L, Zhang C, Xie Y and Jiang Y: SERCA3Role of in the prognosis and immune function in Pan-cancer. J Oncol 2022: 9359879, 2022.
36. Song J, Yang R, Wei R, Du Y, He P and Liu X: Pan-cancer analysis reveals RIPK2 predicts prognosis and promotes immune therapy resistance via triggering cytotoxic T lymphocytes dysfunction. Mol Med 28: 47, 2022.
37. Fang Z, Li P, Li H, Chong W, Li L, Shang L and Li F: New insights into PTBP3 in human cancers: Immune cell infiltration, TMB, MSI, PDCD1 and m6A markers. Front Pharmacol 13: 811338, 2022.
38. Rossini E, Biscetti F, Rando MM, Nardella E, Cecchini AL, Nicolazzi MA, Covino M, Gasbarrini A, Massetti M and Flex A: Statins in high cardiovascular risk patients: Do comorbidities and characteristics matter? Int J Mol Sci 23: 9326, 2022.
39. Zhou E, Ge X, Nakashima H, Li R, van der Zande HJP, Liu C, Li Z, Müller C, Bracher F, Mohammed Y, *et al*: Inhibition of DHCR24 activates LXRα to ameliorate hepatic steatosis and inflammation. EMBO Mol Med 15: e16845, 2023.
40. Bravi F, Scotti L, Bosetti C, Talamini R, Negri E, Montella M, Franceschi S and La Vecchia C: Self-reported history of hypercholesterolaemia and gallstones and the risk of prostate cancer. Ann Oncol 17: 1014-1017, 2006.
41. Murtola TJ, Kasurinen TVJ, Talala K, Taari K, Tammela TLJ and Auvinen A: Serum cholesterol and prostate cancer risk in the Finnish randomized study of screening for prostate cancer. Prostate Cancer Prostatic Dis 22: 66-76, 2019.
42. Yang L, Sun J, Li M, Long Y, Zhang D, Guo H, Huang R and Yan J: Oxidized Low-density lipoprotein links hypercholesterolemia and bladder cancer aggressiveness by promoting cancer stemness. Cancer Res 81: 5720-5732, 2021.
43. Glaser S, Hsu J and Gulley M: Epstein-Barr virus and breast cancer: State of the evidence for viral carcinogenesis. Cancer Epidemiol Biomarkers Prev 13: 688-697, 2004.
44. Liang Q, Yao X, Tang S, Zhang J, Yau TO, Li X, Tang CM, Kang W, Lung RW, Li JW, *et al*: Integrative identification of Epstein-Barr virus-associated mutations and epigenetic alterations in gastric cancer. Gastroenterology 147: 350-1362.e4, 2014.
45. Glaviano A, Foo ASC, Lam HY, Yap KCH, Jacot W, Jones RH, Eng H, Nair MG, Makvandi P, Geoerger B, *et al*: PI3K/AKT/mTOR signaling transduction pathway and targeted therapies in cancer. Mol Cancer 22: 138, 2023.
46. Rezaei S, Nikpanjeh N, Rezaee A, Gholami S, Hashemipour R, Biavarz N, Yousefi F, Tashakori A, Salmani F, Rajabi R, *et al*: PI3K/Akt signaling in urological cancers: Tumorigenesis function, therapeutic potential, and therapy response regulation. Eur J Pharmacol 955: 175909, 2023.
47. Houédé N and Pourquier P: Targeting the genetic alterations of the PI3K-AKT-mTOR pathway: Its potential use in the treatment of bladder cancers. Pharmacol Ther 145: 1-18, 2015.
48. Zhang Y and Zhang Z: The history and advances in cancer immunotherapy: Understanding the characteristics of tumor-infiltrating immune cells and their therapeutic implications. Cell Mol Immunol 17: 807-821, 2020.
49. Sordo-Bahamonde C, Lorenzo-Herrero S, Granda-Díaz R, Martínez-Pérez A, Aguilar-García C, Rodrigo JP, García-Pedrero JM and Gonzalez S: Beyond the anti-PD-1/PD-L1 era: Promising role of the BTLA/HVEM axis as a future target for cancer immunotherapy. Mol Cancer 22: 142, 2023.
50. Cox A and Der C: Ras history: The saga continues. Small GTPases 1: 2-27, 2010.
51. Coley AB, Ward A, Keeton AB, Chen X, Maxuitenko Y, Prakash A, Li F, Foote JB, Buchsbaum DJ and Piazza GA: Pan-RAS inhibitors: Hitting multiple RAS isozymes with one stone. Adv Cancer Res 153: 131-168, 2022.
52. McCormick F: A brief history of RAS and the RAS initiative. Adv Cancer Res 153: 1-27, 2022.
53. Li D, Jackson RA, Yusoff P and Guy GR: Direct association of Sprouty-related protein with an EVH1 domain (SPRED) 1 or SPRED2 with DYRK1A modifies substrate/kinase interactions. J Biol Chem 285: 35374-35385, 2010.
54. Cerami E, Gao J, Dogrusoz U, Gross BE, Sumer SO, Aksoy BA, Jacobsen A, Byrne CJ, Heuer ML, Larsson E, *et al*: The cBio cancer genomics portal: An open platform for exploring multidimensional cancer genomics data. Cancer Discov 2: 401-404, 2012.
55. Gao J, Aksoy BA, Dogrusoz U, Dresdner G, Gross B, Sumer SO, Sun Y, Jacobsen A, Sinha R, Larsson E, *et al*: Integrative analysis of complex cancer genomics and clinical profiles using the cBioPortal. Sci Signal 6: pl1, 2013.
56. Prior I, Hood F and Hartley J: The frequency of ras mutations in cancer. Cancer Res 80: 2969-2974, 2020.
57. Zehir A, Benayed R, Shah RH, Syed A, Middha S, Kim HR, Srinivasan P, Gao J, Chakravarty D, Devlin SM, *et al*: Mutational landscape of metastatic cancer revealed from prospective clinical sequencing of 10,000 patients. Nat Med 23: 703-713, 2017.
58. Kodaz H, Kostek O, Hacioglu MB, Erdogan B, Kodaz CE, Hacibekiroglu I, Turkmen T, Uzunoglu S and Cicin I: Frequency of RAS mutations (KRAS, NRAS, HRAS) in human solid cancer. EJMO 1: 1–7, 2017.
59. Prior I, Lewis P and Mattos C: A comprehensive survey of Ras mutations in cancer. Cancer Res 72: 2457-2467, 2012.
60. Skubic C, Trček H, Nassib P, Kreft T, Walakira A, Pohar K, Petek S, Režen T, Ihan A and Rozman D: Knockouts of CYP51A1, DHCR24, or SC5D from cholesterol synthesis reveal pathways modulated by sterol intermediates. iScience 27: 110651, 2024.
61. Daniel H, Holger AS, Klaus A, Andreas H and Peter M: Desmosterol may replace cholesterol in lipid membranes. Biophys J 88: 1838-1844, 2005.
62. Lu X, Kambe F, Cao X, Yoshida T, Ohmori S, Murakami K, Kaji T, Ishii T, Zadworny D and Seo H: DHCR24-knockout embryonic fibroblasts are susceptible to serum withdrawal-induced apoptosis because of dysfunction of caveolae and insulin-Akt-Bad signaling. Endocrinology 147: 3123-3132, 2006.
63. Lu X, Kambe F, Cao X, Kozaki Y, Kaji T, Ishii T and Seo H: 3beta-Hydroxysteroid-delta24 reductase is a hydrogen peroxide scavenger, protecting cells from oxidative stress-induced apoptosis. Endocrinology 149: 3267-3273, 2008.

64. Relovska S, Wang H, Zhang X, Fernández-Tussy P, Jeong KJ, Choi J, Suárez Y, McDonald JG, Fernández-Hernando C and Chung JJ: DHCR24-mediated sterol homeostasis during spermatogenesis is required for sperm mitochondrial sheath formation and impacts male fertility over time. bioRxiv: Feb 11, 2024 doi: 10.1101/2023.12.21.572851.
65. Hengbing Z, Junfeng W, Jianfeng Z, Min Y and Zhen H: Testosterone up-regulates seladin-1 expression by iAR and PI3-K/Akt signaling pathway in C6 cells. Neurosci Lett 514: 122-126, 2012.
66. Legg RL, Tolman JR, Lovinger CT, Lephart ED, Setchell KD and Christensen MJ: Diets high in selenium and isoflavones decrease androgen-regulated gene expression in healthy rat dorsolateral prostate. Reprod Biol Endocrinol 6: 57, 2008.
67. Nakken HL, Lephart ED, Hopkins TJ, Shaw B, Urie PM and Christensen MJ: Prenatal exposure to soy and selenium reduces prostate cancer risk factors in tramp mice more than exposure beginning at six weeks. Prostate 76: 588-596, 2016.
68. Wei H, Li Z, Qian K, Du W, Ju L, Shan D, Yu M, Fang Y, Zhang Y, Xiao Y, *et al*: Unveiling the association between HMG-CoA reductase inhibitors and bladder cancer: A comprehensive analysis using mendelian randomization, animal models, and transcriptomics. Pharmacogenomics J 24: 24, 2024.
69. Yang X, Wang L, Lin P, Ning Y, Lin Y, Xie Y, Zhao C, Mu L and Xu C: Discovery of artesunate (ARS) PROTACs as GPX4 protein degraders for the treatment of bladder cancer. Eur J Med Chem 293: 117710, 2025.